A method for estimating and assessing modes of interannual variability in coupled climate models

S. Grainger[1] C. S. Frederiksen[2] X. Zheng[3]

(Received 20 March 2015; revised 31 January 2016)

Abstract

The seasonal mean of a climate variable consists of: slow-external; slow-internal; and intraseasonal components. Using an analysis of variance-based method, the interannual variability of the seasonal mean from an ensemble of coupled atmosphere-ocean general circulation model (CGCM) realisations is separable into these three components. Eigenvalue decomposition is applied to the covariance matrices to obtain, for each component, the dominant modes of variability (eigenvectors) and their associated variance (eigenvalues) for the climate variable. Here, a method is described that assesses the modes of interannual variability in CGCMs against those obtained from reanalysis data based on observations. A metric is defined based on the pattern correlation

http://journal.austms.org.au/ojs/index.php/ANZIAMJ/article/view/9445 gives this article, Published February 17, 2016, as part of the Proceedings of the 17th Biennial Computational Techniques and Applications Conference. ISSN 1446-8735.

between the observed and modelled modes of variability, and the ratio of their associated variances. This metric is applied to monthly mean southern hemisphere 500 hPa geopotential height from the second half of the 20th century. It is shown that CGCMs have clear differences in the slow-component of modes of interannual variability, related to external forcings and/or slowly-varying internal variability.

Contents

1 Introduction

The variability of the atmospheric circulation is controlled by many physical processes, which may act on time scales ranging from days to years. These processes, on their different timescales, influence the interannual variability of the seasonal mean of a climate variable [1]. Consequently, a seasonal mean climate anomaly is considered as a statistical random variable consisting of signal and noise components [2]. The signal is related to slowly varying (a season or longer) processes and is considered the slow component of interannual variability of the seasonal mean [3]. In a coupled atmosphere-ocean climate system, this signal may be due to either slowly varying internal dynamics, or to changes in external forcing, for example, changing greenhouse gas concentrations. The noise is related to internal dynamics with intraseasonal time scales of about 14–90 days. Zheng and Frederiksen [3] referred to this noise as the intraseasonal component of the seasonal mean.

Zheng and Frederiksen [3] formulated a method for estimating the statistical modes of interannual covariability of the slow and intraseasonal components. Using monthly mean data, the interannual covariability of the seasonal mean was estimated by second moments. The application of the seasonal mean operator separated the signal and noise components, and the result was equivalent to using raw daily data, filtered or unfiltered [1].

Frederiksen and Zheng [4] applied the method of Zheng and Frederiksen [3] to the southern hemisphere 500 hPa geopotential height field in reanalysis data. They found that the leading modes, or coherent patterns, of the slow component of interannual variability were associated with the High Latitude Mode, and with the atmospheric response to the El Niño-southern oscillation (ENSO). Grainger et al. [5] developed a method to assess these modes of interannual variability in coupled atmosphere-ocean general circulation models (CGCMs) from the World Climate Research Program (WCRP) Coupled Model Intercomparison Project phase 3 (CMIP3) dataset [6]. In this article, we extend the previous analysis to CGCMs in the more recent Coupled Model Intercomparison Project phase 5 (CMIP5) dataset [7]. The performance of CGCMs between the two datasets is examined, and a new metric is defined to give an overall ranking of model performance.

2 Separation of variability

Given the conceptual model described in Section 1, the separation of the interannual variability of the seasonal mean into signal and noise components is possible given at least monthly data [1, 8]. Here, we assume that we have monthly mean data on a spatial grid for an ensemble of model realisations. In this case, after the annual cycle is removed, the monthly mean anomaly of a climate variable x at any grid point is [8]

$$x_{sym} = \beta_y + \delta_{sy} + \varepsilon_{sym}\,, \tag{1}$$

where $s = 1, \ldots, S$ is the realisation number in an ensemble of size S, $y = 1, \ldots, Y$ is the year index in a sample of Y years and $m = 1, 2, 3$ is the month index in a season. The slow-external component, independent of realisation, is β_y, δ_{sy} is the slow-internal component, taken to be constant over a season, and the intraseasonal component ε_{sym} is the residual monthly departure of x_{sym} from the slow components. Here, we are interested in the time series of the slow component, that is,

$$\mu_{sy} = \beta_y + \delta_{sy}\,. \tag{2}$$

Zheng and Frederiksen [3] showed that it is possible to estimate covariance matrices for the slow and intraseasonal components of the interannual variability of the seasonal mean. The total seasonal mean covariance is estimated as the sum of the covariances of the external and internal components [8], that is,

$$\hat{V}(x^1_{sy\circ}, x^2_{sy\circ}) = \hat{V}(\beta^1_y, \beta^2_y) + \hat{V}(\delta^1_{sy} + \varepsilon^1_{sy\circ}, \delta^2_{sy} + \varepsilon^2_{sy\circ})\,, \tag{3}$$

where x^1_{sym} and x^2_{sym} are the time series at any two grid points in the set $i = 1, \ldots, I$, the subscript $\circ$ denotes an average over an index s, y or m, and $\hat{V}$ denotes an estimated covariance. Total internal covariance is estimated by

$$\hat{V}(\delta^1_{sy} + \varepsilon^1_{sy\circ}, \delta^2_{sy} + \varepsilon^2_{sy\circ}) = \frac{1}{Y(S-1)} \sum_{y=1}^{Y} \sum_{s=1}^{S} \left(x^1_{sy\circ} - x^1_{\circ y\circ}\right) \left(x^2_{sy\circ} - x^2_{\circ y\circ}\right), \tag{4}$$

and the covariance of the slow-external component by

$$\hat{V}(\beta^1_y, \beta^2_y) = \hat{V}(x^1_{\circ y\circ}, x^2_{\circ y\circ}) - \frac{1}{S}\hat{V}(\delta^1_{sy} + \varepsilon^1_{sy\circ}, \delta^2_{sy} + \varepsilon^2_{sy\circ})\,, \tag{5}$$

where

$$\hat{V}(x^1_{oyo}, x^2_{oyo}) = \frac{1}{Y-1} \sum_{y=1}^{Y} \left(x^1_{oyo} - x^1_{ooo}\right) \left(x^2_{oyo} - x^2_{ooo}\right) \tag{6}$$

is the ensemble mean seasonal mean covariance. In the special case of a single model realisation, that is $S = 1$, it is not possible to separately estimate the external and internal covariances; instead, the total seasonal mean covariance is estimated directly from equation (6).

For the intraseasonal component, Zheng and Frederiksen [3] showed that the covariance is able to be estimated as a function of monthly moments. In this case,

$$\hat{V}(\varepsilon^1_{syo}, \varepsilon^2_{syo}) = \frac{1}{9} \left[\hat{\alpha}(3 + 4\hat{\phi})\right], \tag{7}$$

where

$$\hat{\alpha} = a/[2(1 - \hat{\phi})] \tag{8}$$

is the covariance of the intraseasonal components within each month, and

$$\hat{\phi} = (a + 2b)/[2(a + b)], \quad 0 \leqslant \hat{\phi} \leqslant 0.1, \tag{9}$$

is the intermonthly correlation between consecutive months. The covariance and intermonth correlations of the intraseasonal components are assumed to be independent of months within a season. The two monthly moments are

$$\begin{aligned} a &= \frac{1}{2} \left[\frac{1}{YS} \sum_{y=1}^{Y} \sum_{s=1}^{S} \left(x^1_{sy1} - x^1_{sy2}\right) \left(x^2_{sy1} - x^2_{sy2}\right) \right. \\ &\qquad \left. + \frac{1}{YS} \sum_{y=1}^{Y} \sum_{s=1}^{S} \left(x^1_{sy2} - x^1_{sy3}\right) \left(x^2_{sy2} - x^2_{sy3}\right) \right], \end{aligned} \tag{10}$$

$$\begin{aligned} b &= \frac{1}{2} \left[\frac{1}{YS} \sum_{y=1}^{Y} \sum_{s=1}^{S} \left(x^1_{sy1} - x^1_{sy2}\right) \left(x^2_{sy2} - x^2_{sy3}\right) \right. \\ &\qquad \left. + \frac{1}{YS} \sum_{y=1}^{Y} \sum_{s=1}^{S} \left(x^1_{sy2} - x^1_{sy3}\right) \left(x^2_{sy1} - x^2_{sy2}\right) \right]. \end{aligned} \tag{11}$$

The interannual covariance of the slow component is defined as the residual of the total seasonal mean covariance after the removal of the covariance of the intraseasonal component, that is,

$$\hat{V}(\mu^1_{sy}, \mu^2_{sy}) = \hat{V}(x^1_{syo}, x^2_{syo}) - \hat{V}(\epsilon^1_{syo}, \epsilon^2_{syo})\,. \tag{12}$$

For all components, $(I \times I)$ covariance matrices are obtained by applying equations (3), (7) and (12) to all pairs of grid points. The modes of interannual variability of each component are defined as the empirical orthogonal functions (EOFs) obtained by eigenvalue decomposition of the corresponding covariance matrix, in descending order by variance explained [9]. The leading eigenvectors give the dominant modes of variability for each component, and the corresponding eigenvalues give the estimated variance associated with each mode.

3 Model assessment

The centred mean square difference between reference and model samples is [5]

$$E' = \hat{V} + \hat{V}' - 2\sqrt{\hat{V}}\sqrt{\hat{V}'}C\,, \tag{13}$$

where C is the correlation between the two samples, and $\hat{V}$ and $\hat{V}'$ are the estimated reference and model sample variances, respectively, for example the EOF associated variances defined in Section 2. Based on this, Grainger et al. [10] proposed a score for how well a CGCM reproduces the jth reference slow component mode of variability (slow-EOF):

$$M^j_\mu = \frac{|R^j|\left(1 + R^j_{sst}\right)^2}{2\left(\frac{\hat{V}'_\mu}{\hat{V}_\mu} + \frac{\hat{V}_\mu}{\hat{V}'_\mu}\right)}\,, \tag{14}$$

where R^j is the pattern correlation between the model and reference slow-EOFs and R^j_{sst} is the pattern correlation between the model and reference slow sea surface temperature (SST)–height covariance patterns. The method for calculating the slow SST–height covariance patterns is analogous to the covariance methodology in Section 2, and is detailed by Grainger et al. [11].

The application of equation (14) requires a one to one match between model and reference slow-EOFs. This is obtained by the following procedure.

1. For the leading J reference slow-EOFs, find the permutation of the leading J model slow-EOFs which maximises
$$\sum_{j=1}^{J} |R^j| \left(1 + R^j_{sst}\right)^2 .$$
2. For each $j = 1, \ldots, J$ reference mode, first check for higher order, that is, $> J$ model modes with a higher score $M'_\mu > M^j_\mu$. Then check *all* model modes for ambiguous scores, defined as $M'_\mu \geqslant 0.75 M^j_\mu$.
3. If higher order or ambiguous modes are identified, manually inspect the model slow-EOFs to resolve the one to one match.

4 Application

To illustrate the methodology, slow-EOFs of 500 hPa geopotential height for the southern hemisphere summer (December-January-February, DJF) and winter (June-July-August, JJA) are examined. CGCM data were obtained from the WCRP CMIP3 [6] and CMIP5 [7] multi-model datasets. Data from the Twentieth Century Reanalysis Project (20CR) [12] for the period 1951–2000 was used as the reference dataset. Observed SST data were obtained from the HADISST dataset [13]. All 500 hPa geopotential height data were mapped to a 2.5° × 2.5° latitude/longitude grid, and SST data to a 2° × 2° latitude/longitude grid.

Figure 1: (a) Leading three slow-EOFs (normalised to unit length) of 20CR southern hemisphere 500 hPa geopotential height for DJF for the period 1951–2000. (b) Slow SST–height covariance (m K) with HADISST SST for the slow-EOFs in (a). The estimated standard deviation (m) and variance explained (%) are given bottom left in (a) for each EOF.

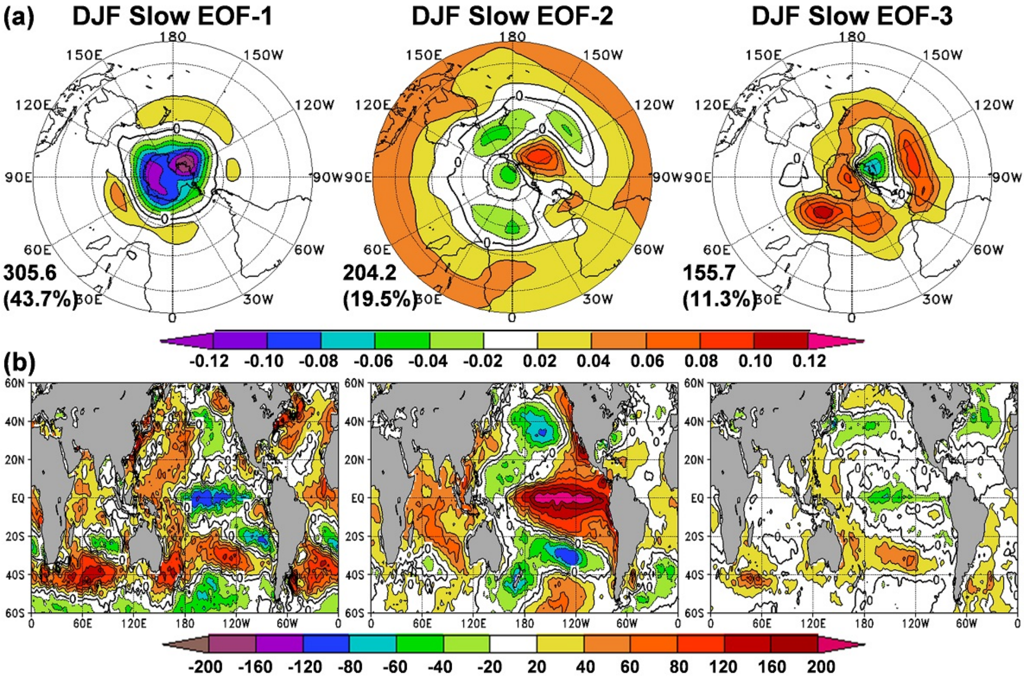

The leading three slow-EOFs of 20CR southern hemisphere 500 hPa geopotential height in DJF and JJA are shown in Figures 1 and 2, respectively. In both seasons, the leading slow-EOF represents high latitude variability associated with the southern annular mode [4]. There is a protrusion into the South Pacific, particularly in JJA (Figure 2(a)). Slow-EOFs 2 and 3 in both seasons represent variability associated with ENSO [4], evident in the slow SST–height covariances (Figures 1(b) and 2(b)), which show a strong relationship with tropical Pacific SSTs.

Figure 2: (a) Leading three slow-EOFs (normalised to unit length) of 20CR southern hemisphere 500 hPa geopotential height for JJA for the period 1951–2000. (b) Slow SST–height covariance (m K) with HADISST SST for the slow-EOFs in (a. The estimated standard deviation (m) and variance explained (%) are given bottom left in (a) for each EOF.

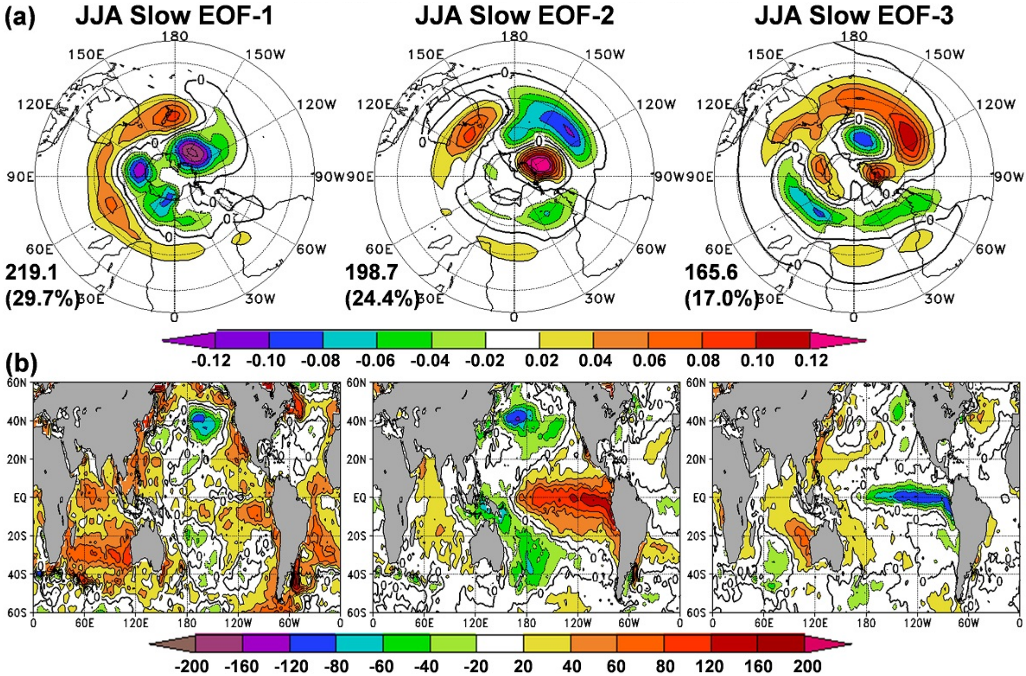

The matching slow-EOFs were estimated for the same period using the ensemble over all realisations for each of the 23 CMIP3 and 45 CMIP5 models which were available. The model slow-EOFs were then evaluated against the 20CR slow-EOFs (see Section 3) using $J = 3$. For each season, an overall score is calculated by

$$M_\mu^{sss} = \frac{1}{3}\sum_{j=1}^{3} M_\mu^j \,, \qquad (15)$$

where sss denotes a season, that is DJF or JJA. The overall scores thus calculated are shown in Figure 3 for all models for both seasons. In order to rank the CGCMs, a weighting based on their relative spread within each season is used, that is,

$$M_{\mu}^{\mathrm{tot}} = M_{\mu}^{\mathrm{djf}} + 2.2 M_{\mu}^{\mathrm{jja}} . \tag{16}$$

In DJF (Figure 3(a)), there is fairly consistent performance across most models, with many models having an overall score > 0.4. In contrast, the CGCMs reproduce the 20CR JJA slow-EOFs (Figure 2) less well, with only two CGCMs having an overall score > 0.4. Figure 3 also shows that the performance of CMIP5 CGCMs has improved relative to CMIP3, with generally higher overall scores in both seasons.

5 Conclusions

In this article, a method was formulated to assess the skill of climate models in reproducing the leading slowly varying modes of interannual variability of the seasonal mean. The method was applied to southern hemisphere 500 hPa geopotential height. Coherent spatial patterns, reperesented by the slow-EOFs, of interannual variability for summer (DJF) and winter (JJA) were estimated for the CMIP5 and CMIP3 datasets for the period 1951–2000. These were assessed against reference slow-EOFs from 20CR data for the same period.

The 20CR slow-EOFs are best reproduced in DJF. The slow-EOFs are less well reproduced in JJA. The spread of results in both seasons enables the definition of a metric ranking model overall performance. There are clear improvements in the CMIP5 dataset over CMIP3 during both summer and winter. The largest individual improvements (not shown) in CMIP5 CGCMs are in the spatial structures of the slow-EOFs related to ENSO variability and their slow SST–height covariances.

The method developed in this article is generally applicable to any climate variable for which the interannual variability of the components are separable.

Figure 3: Model overall score (equation (15)) for (a) DJF and (b) JJA for all CMIP3 (blue) and CMIP5 (red) CGCMS. Models are shown in order of the total overall score (equation (16)).

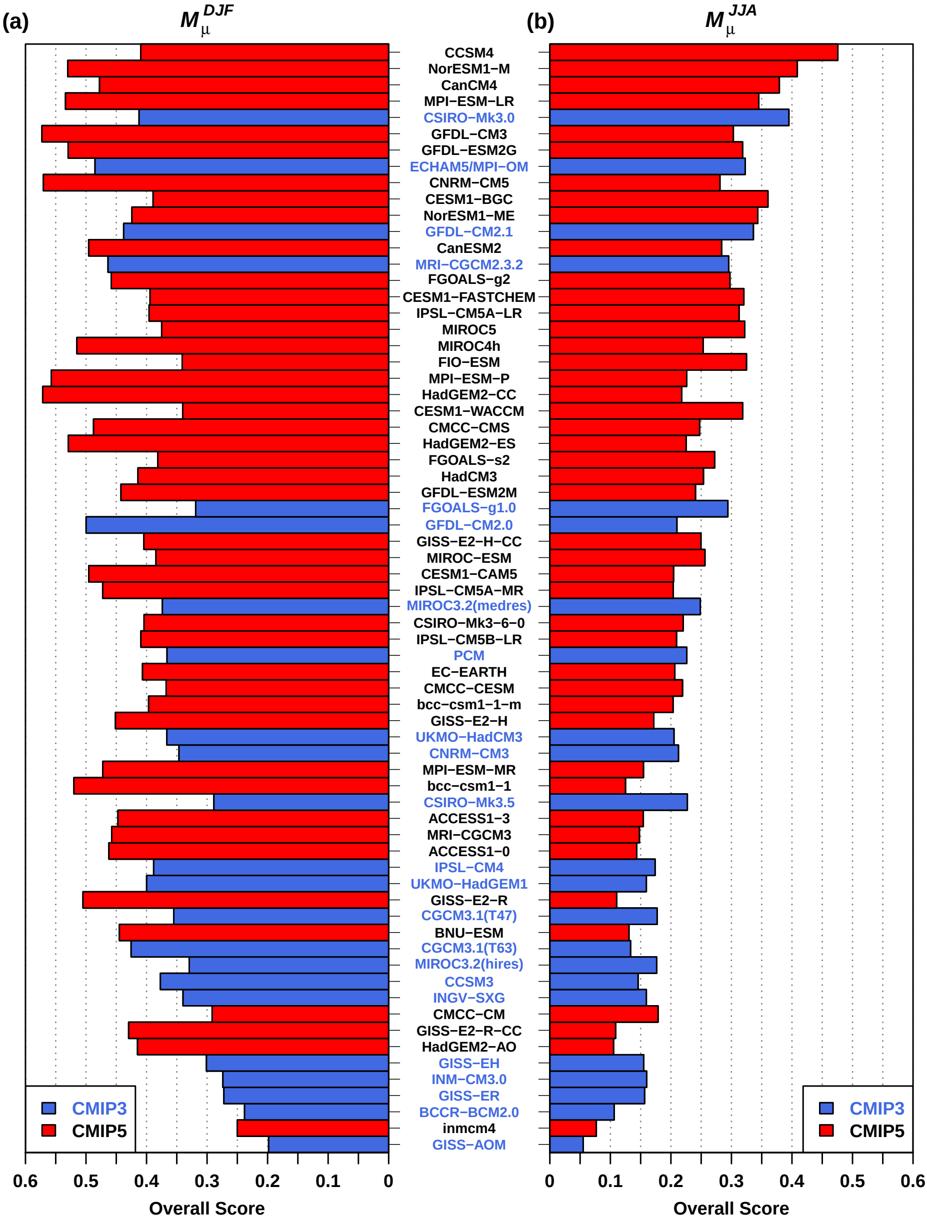

The slow-EOFs of northern hemisphere 500 hPa geopotential height in CMIP5 models will be assessed. The method is able to track improvements in the interannual variability of future multi-model datasets as they become available.

Acknowledgements We acknowledge the modelling groups, the Program for Climate Model Diagnosis and Intercomparison and the WCRP's Working Group on Coupled Modeling for their roles in making available the CMIP3 and CMIP5 multi-model datasets. This work is partially supported by the Australian Climate Change Science Program of the Australian Department of the Environment.

References

[1] C. S. Frederiksen and X. Zheng. Coherent structures of interannual variability of the atmospheric circulation: the role of intraseasonal variability. *Frontiers in Turbulence and Coherent Structures*, *World Scientific Lecture Notes in Complex Systems*, Vol. 6, Eds Jim Denier and Jorgen Frederiksen, World Scientific Publications, 87–120, 2007. doi:10.1142/6320 C370, C371

[2] C. E. Leith. The standard error of time-average estimates of climatic means. *J. Appl. Meteor.*, 12:1066–1069, 1973. doi:10.1175/1520-0450(1973)012<1066:TSEOTA>2.0.CO;2 C370

[3] X. Zheng and C. S. Frederiksen. Variability of seasonal-mean fields arising from intraseasonal variability: part 1, methodology. *Clim. Dynam.*, 23:177–191, 2004. doi:10.1007/s00382-004-0428-7 C370, C371, C372, C373

[4] C. S. Frederiksen and X. Zheng. Variability of seasonal-mean fields arising from intraseasonal variability. Part 3: Application to SH winter

and summer circulations. *Clim. Dynam.*, 28:849–866, 2007. doi:10.1007/s00382-006-0214-9 C371, C376

[5] S. Grainger, C. S. Frederiksen and X. Zheng. A method for evaluating the modes of variability in general circulation models. *ANZIAM J.*, 50:C399–C412, 2008. http://journal.austms.org.au/ojs/index.php/ANZIAMJ/article/view/1431 C371, C374

[6] G. A. Meehl, C. Covey, K. E. Taylor, T. Delworth, R. J. Stouffer, M. Latif, B. McAvaney and J. F. B. Mitchell. The WCRP CMIP3 multimodel dataset: A new era in climate change research. *Bull. Amer. Meteor. Soc.*, 88:1383–1394, 2007. doi:10.1175/BAMS-88-9-1383 C371, C375

[7] K. E. Taylor, R. J. Stouffer and G. A. Meehl. An overview of CMIP5 and the experiment design. *Bull. Amer. Meteor. Soc.* 93:485–498, 2012. doi:10.1175/BAMS-D-11-00094.1 C371, C375

[8] X. Zheng, M. Sugi and C. S. Frederiksen. Interannual variability and predictability in an ensemble of climate simulations with the MRI-JMA AGCM. *J. Meteor. Soc. Jap.*, 82:1–18, 2004. doi:10.2151/jmsj.82.1 C371, C372

[9] H. von Storch and F. W. Zwiers. Statistical Analysis in Climate Research. *Cambridge University Press*, 484pp, 1999. doi:10.1017/cbo9780511612336 C374

[10] S. Grainger, C. S. Frederiksen and X. Zheng. Modes of interannual variability of Southern Hemisphere atmoshperic circulation in CMIP3 models: assessment and projections. *Clim. Dynam.* 41:479–500, 2013. doi:10.1007/s00382-012-1659-7 C374

[11] S. Grainger, C. S. Frederiksen and X. Zheng. Estimating components of covariance between two climate variables using model ensembles. *ANZIAM J.*, 52:C318–C332, 2011. http://journal.austms.org.au/ojs/index.php/ANZIAMJ/article/view/3928 C375

[12] G. P. Compo, J. S. Whitaker, P. D. Sardeshmukh, N. Matsui, R. J. Allan, X. Yin, B. E. Gleason, R. S. Vose, G. Rutledge, P. Bessemoulin, S. Bronnimann, M. Brunet, R. I. Crouthamel, A. N. Grant, P. Y. Groisman, P. D. Jones, M. C. Kruk, A. C. Kruger, G. J. Marshall, M. Maugeri, H. Y. Mok, O. Nordli, T. F. Ross, R. M. Trigo, X. L. Wang, S. D. Woodruff and S. J. Worley. The Twentieth Century Reanalysis Project. *Quart. J. Roy. Meteor. Soc.* 137:1–28, 2011. doi:10.1002/qj.776 C375

[13] N. A. Rayner, D. E. Parker, E. B. Horton, C. K. Folland, L. V. Alexander, D. P. Rowell, E. C. Kent and A. Kaplan. Global analyses of sea surface temperature, sea ice, and night marine air temperature since the late nineteenth century. *J. Geophys. Res.*, 108(D14):4407, 2003. doi:10.1029/2002JD002670 C375

Author addresses

1. **S. Grainger**, Environment and Research Division, Bureau of Meteorology, Melbourne, Victoria 3001, Australia.
2. **C. S. Frederiksen**, Environment and Research Division, Bureau of Meteorology, Melbourne, Victoria 3001, Australia. `mailto:c.frederiksen@bom.gov.au`
3. **X. Zheng**, College of Global Change and Earth System Science, Beijing Normal University, Beijing, China.